Synthesis and Characterization of $MO[OSi(O^tBu)_3]_4$ and $MO_2[OSi(O^tBu)_3]_2$ (M = Mo, W): Models for Isolated Oxo-Molybdenum and -Tungsten Sites on Silica and Precursors to Molybdena− and Tungsta−Silica Materials

Jonggol Jarupatrakorn, Martyn P. Coles,† and T. Don Tilley*

Department of Chemistry, University of California, Berkeley, California 94720-1460, and the Chemical Sciences Division, Lawrence Berkeley National Laboratory, 1 Cyclotron Road, Berkeley, California 94720

Received May 20, 2004. Revised Manuscript Received January 20, 2005

The tri(alkoxy)siloxy complexes $MO[OSi(O^tBu)_3]_4$ (**1**, M = Mo and **2**, M = W) were prepared from $MOCl_4$ and $LiOSi(O^tBu)_3$. Similarly, reactions of $MO_2Cl_2(DME)$ with $LiOSi(O^tBu)_3$ afforded the new siloxide complexes $MO_2[OSi(O^tBu)_3]_2$ (**3**, M = Mo and **4**, M = W), which are themally unstable at ambient temperature. More stable compounds were obtained by the crystallizations of **3** and **4** in a coordinating solvent, to form the ether adducts $MoO_2[OSi(O^tBu)_3]_2(THF)$ (**3a**) and $WO_2[OSi(O^tBu)_3]_2$-(DME) (**4a**). These compounds serve as soluble models for isolated molybdenum or tungsten atoms on a silica surface and were characterized by ^1H, ^{13}C, ^{29}Si, ^{95}Mo, and ^{183}W NMR, FT-Raman, FT-IR, and UV−vis spectroscopies. Compounds **1**, **2**, **3a**, and **4a** were used to prepare metal−oxide silica composites via the thermolytic molecular precursor method. The xerogels obtained from the thermolyses of **1**, **2**, **3a**, and **4a** in toluene contained mesoporosity with surface areas of 10, 230, 106, and 270 $m^2\ g^{-1}$, respectively. Despite the high surface areas for most samples, these xerogels contain MO_3 domains. Complexes **1** and **2** were also used to introduce molybdenum and tungsten sites, respectively, onto mesoporous SBA-15 silica via displacement of the $-OSi(O^tBu)_3$ ligand for a siloxyl group from the silica surface. All molybdenum- and tungsten-containing systems were tested as catalysts for the epoxidation of cyclohexene using *tert*-butyl hydroperoxide (TBHP) or aqueous H_2O_2 as the oxidant.

Introduction

Surface-bound oxo-molybdenum and -tungsten species have attracted considerable attention in recent years because of their relevance to a variety of catalytic reactions, including the selective oxidations of alkanes,[1,2] alkenes,[3] and alcohols.[4,5] Many research groups have reported synthetic methods which are proposed to generate a specific surface molybdenum and tungsten oxide species. At low coverage, the active sites have been proposed to have various structures, including isolated dioxo surface species,[4,6−9] isolated mono-oxo species,[10−13] and dimeric surface species[14] (Scheme 1).

Several oxo-molybdenum and -tungsten complexes with various supporting siloxide ligands, such as $MoO_2(OSiPh_3)_2$,[15] $MoO_2(OSiMe_2{}^tBu)_2(py)$,[16] $[O_2Mo(O_2Si{}^tBu_2)]_2$,[17] $MoO_2[(c\text{-}C_6H_{11})_7(Si_7O_{12})(OSiMe_3)]$,[18] $WO[O(Ph_2SiO)_3]_2(THF)$, and $WO_2(OSiPh_3)_2(OSC_4H_8)_2$,[19] have been reported as models for the active sites of molybdenum- and tungsten-containing oxotransfer catalysts. Although these molecular species represent interesting structural models for isolated oxo-molybdenum and -tungsten sites on silica, the presence of the organic substituents on silicon complicates the direct comparison of spectroscopic data with molybdena− and tungsta−silica catalysts.

Our research has focused on the synthesis of single-source molecular precursors to mixed-element oxides.[20−30] For this

* To whom correspondence should be sent. E-mail: tdtilley@berkeley.edu.
† Current address: Department of Chemistry, University of Sussex, Falmer, Brighton, BN1 9RH U.K.

(1) Spencer, N. D.; Pereira, C. J.; Grasselli, R. K. *J. Catal.* **1990**, *126*, 546.
(2) Banares, M. A.; Fierro, J. L. G.; Moffat, J. B. *J. Catal.* **1993**, *142*, 406.
(3) Giordano, N.; Meazzo, M.; Castellan, A.; Bart, J. C.; Ragaini, V. *J. Catal.* **1977**, *50*, 342.
(4) Louis, C.; Tatibouet, J. M.; Che, M. *J. Catal.* **1988**, *109*, 354.
(5) Ono, T.; Anpo, M.; Kubokawa, Y. *J. Phys. Chem.* **1986**, *90*, 4780.
(6) Desikan, A. N.; Oyama, S. T. *J. Chem. Soc., Chem. Commun.* **1992**, *88*, 3357.
(7) Takenaka, S.; Tanaka, T.; Funabiki, T.; Yoshida, S. *J. Phys. Chem. B* **1998**, *102*, 2960.
(8) Kim, D. S.; Ostromecki, M.; Wach, I. E.; Kohler, S. D.; Ekerdt, J. G. *Catal. Lett.* **1995**, *33*, 209.
(9) Kim, D. S.; Ostromecki, M.; Wachs, I. E. *J. Mol. Catal. A* **1996**, *106*, 93.
(10) de Boer, M.; van Dillen, A. J.; Koningsberger, D. C.; Geus, J. W.; Vuurman, M. A.; Wachs, I. E. *Catal. Lett.* **1991**, *11*, 227.
(11) Williams, C. C.; Ekerdt, J. G.; Jehng, J.-M.; Hardcastle, F. D.; Turek, A. M.; Wachs, I. E. *J. Phys. Chem.* **1991**, *95*, 8781.
(12) Louis, C.; Che, M.; Anpo, M. *J. Catal.* **199**3, *141*, 453.
(13) Banares, M. A.; Hu, H.; Wachs, I. E. *J. Catal.* **1994**, *150*, 407.
(14) Iwasawa, Y. *Adv. Catal.* **1987**, *35*, 265.
(15) Huang, M.; DeKock, C. W. *Inorg. Chem.* **1993**, *32*, 2287.
(16) Kim, G.-S.; Huffman, D.; DeKock, C. W. *Inorg. Chem.* **1989**, *28*, 1279.
(17) Gosink, H.-J.; Roesky, H. W.; Noltemeyer, M.; Schmidt, H.-G.; Freire-Erdbrugger, C.; Sheldrick, G. M. *Chem. Ber.* **1993**, *126*, 279.
(18) Feher, F. J.; Rahimian, K.; Budzichowski, T. A.; Ziller, J. W. *Organometallics* **1995**, *14*, 3920.
(19) Brisdon, B. J.; Mahon, M. F.; Rainford, C. C. *J. Chem. Soc., Dalton Trans.* **1998**, *19*, 3295.
(20) Tilley, T. D. *J. Mol. Catal. A* **2002**, *182−183*, 17.
(21) Fujdala, K. L.; Tilley, T. D. *J. Catal.* **2003**, *216*, 265.
(22) Terry, K. W.; Tilley, T. D. *Chem. Mater.* **1991**, *3*, 1001.
(23) Terry, K. W.; Gantzel, P. K.; Tilley, T. D. *Chem. Mater.* **1992**, *4*, 1290.
(24) Terry, K. W.; Lugmair, C. G.; Gantzel, P. K.; Tilley, T. D. *Chem. Mater.* **1996**, *8*, 274.
(25) Terry, K. W.; Lugmair, C. G.; Tilley, T. D. *J. Am. Chem. Soc.* **1997**, *119*, 9745.

10.1021/cm040344e CCC: $30.25
Published on Web 03/02/2005

Scheme 1

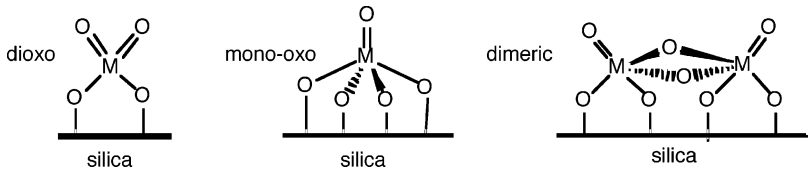

purpose, we have synthesized $MO[OSi(O^tBu)_3]_4$ and $MO_2[OSi(O^tBu)_3]_2$, where M = Mo and W. In related work, Neumann and co-workers generated molybdena− and tungsta−silica materials via the synthetic intermediates $MO[OSi(O^tBu)_3]_4$ (M = Mo and W), which were not isolated or characterized.[31] In this paper, we present details on the synthesis and characterization of $MO[OSi(O^tBu)_3]_4$ and $MO_2[OSi(O^tBu)_3]_2$, which serve as models for mono- and dioxo surface sites (Scheme 1). In addition, we have used the isolated compounds as single-source precursors for the synthesis of molybdena− and tungsta−silica materials, which have been evaluated as catalysts for the epoxidation of cyclohexene.

Aqueous impregnation is the most common method employed for the deposition of molybdenum or tungsten oxide species onto silica.[1,2,11,32] However, in general it is difficult to achieve a high dispersion of the molybdenum or tungsten species with this method.[11] For this reason, there is considerable interest in the development of alternative synthetic methods for the dispersion of molybdenum and tungsten on silica. Many of these methods feature reactions between a labile ligand in a metal complex (such as $MoCl_5$, $Mo(\eta^3\text{-}C_3H_5)_4$, $Mo_2(\eta^3\text{-}C_3H_5)_4$, $Mo_2(OAc)_4$, or $MoO_2(acac)_2$) with the hydroxyl groups on the silica surface.[11,12,14,33−35] As discussed elsewhere, we have shown that the thermolytic molecular precursor route to oxide materials may also be used to introduce catalytic sites onto the surface of a silica support in a controlled manner.[20,21,36,37] In this paper, we describe how this method can be used for the introduction of stable molybdenum and tungsten sites onto a silica surface. The resulting materials have also been investigated as epoxidation catalysts.

Results and Discussion

Synthesis of the Precursor Complexes. The reaction between $MoOCl_4$ and four equivalents of $LiOSi(O^tBu)_3$ in diethyl ether resulted in the elimination of four equivalents of LiCl and formation of $MoO[OSi(O^tBu)_3]_4$ (**1**; eq 1). The product was isolated by evaporation of the solvent under vacuum and was extracted from the LiCl byproduct with pentane. After three recrystallizations from pentane at −30 °C, pale yellow crystals of **1** were isolated in variable yields (10−42%). The analogous reaction with $WOCl_4$ produced $WO[OSi(O^tBu)_3]_4$ (**2**), which was obtained from pentane at −30 °C as a white opaque solid in 39% yield.

$$MOCl_4 + 4LiOSi(O^tBu)_3 \rightarrow MO[OSi(O^tBu)_3]_4 + 4LiCl \qquad M = Mo\ (\mathbf{1}),\ W\ (\mathbf{2}) \quad (1)$$

These compounds are soluble in nonpolar hydrocarbons and hydrolyze very rapidly in air. Room temperature ^1H and ^{13}C NMR spectra for **1** and **2** reveal one resonance for the siloxy ligands. It therefore seems likely that the siloxide ligands are oriented toward the basal corners of a pseudo-square pyramidal coordination geometry, as found for the majority of MOX_4 complexes (M = Mo, W).[38−41]

The addition of a diethyl ether solution of two equivalents of $LiOSi(O^tBu)_3$ to an ether solution of $MoO_2Cl_2(DME)$ at −78 °C produced the complex $MoO_2[OSi(O^tBu)_3]_2$ (**3**). This complex was isolated from pentane at −30 °C as colorless crystals in 30% yield. $WO_2[OSi(O^tBu)_3]_2$ (**4**) was prepared in an analogous way and was isolated as colorless crystals in 52% yield (eq 2).

$$MO_2Cl_2(DME) + 2LiOSi(O^tBu)_3 \rightarrow MO_2[OSi(O^tBu)_3]_2 + 2LiCl \qquad M = Mo\ (\mathbf{3}),\ W\ (\mathbf{4}) \quad (2)$$

Compounds **3** and **4** are air- and temperature-sensitive. Storage in the drybox at room temperature resulted in the decomposition of these complexes within a few hours. To impart further stability, adducts were obtained by recrystallization of **3** and **4** from coordinating solvents. Recrystallization of a sample of **3** in THF afforded $MoO_2[OSi(O^tBu)_3]_2(THF)$ (**3a**). However, the ^1H and ^{13}C NMR spectra of **3a** are identical to those of **3** and contain resonances for free THF. Thus, the THF appears to be largely dissociated in solution. In the solid state, the THF proved to be very labile and could be easily removed under reduced pressure. Recrystallization of a sample of **4** in pentane/DME (1:1) afforded $WO_2[OSi(O^tBu)_3]_2(DME)$ (**4a**). Compounds **3a** and **4a** are also thermally sensitive, but more stable than **3** and **4**. They may be stored in the drybox at room temperature for a few days before

(26) Su, K.; Tilley, T. D. *Chem. Mater.* **1997**, *9*, 588.
(27) Coles, M. P.; Lugmair, C. G.; Terry, K. W.; Tilley, T. D. *Chem. Mater.* **2000**, *12*, 122.
(28) Rulkens, R.; Male, J. L.; Terry, K. W.; Olthof, B.; Khodakov, A.; Bell, A. T.; Iglesia, E.; Tilley, T. D. *Chem. Mater.* **1999**, *11*, 2966.
(29) Kriesel, J. W.; Sanders, M. S.; Tilley, T. D. *Adv. Mater.* **2001**, *13*, 331.
(30) Fujdala, K. L.; Tilley, T. D. *Chem. Mater.* **2001**, *13*, 1817.
(31) Juwiler, D.; Blum, J.; Neumann, R. *Chem. Commun.* **1998**, 1123.
(32) Srinivasan, S.; Datye, A. K. *Catal. Lett.* **1992**, *15*, 155.
(33) Zhuang, Q.; Fukoka, A.; Fujimoto, T.; Tanaka, K.; Ichikawa, M. *J. Chem. Soc., Chem. Commun.* **1991**, *11*, 745.
(34) Ichikawa, M.; Zhuang, Q.; Li, G.-J.; Tanaka, K.; Fujimoto, T.; Fukoka, K. *Stud. Surf. Sci. Catal.* **1992**, *75(A)*, 529.
(35) Collart, O.; Van der Voort, P.; Vansant, E. F.; Gustin, E.; Bouwen, A.; Schoemaker, D.; Ramachandra Rao, R.; Weckhuysen, B. M.; Schoonheydt, R. A. *Phys. Chem. Chem. Phys.* **1999**, 4099.
(36) Jarupatrakorn, J.; Tilley, T. D. *J. Am. Chem. Soc.* **2002**, *124*, 8380.
(37) Nozaki, C.; Lugmair, C. G.; Bell, A. T.; Tilley, T. D. *J. Am. Chem. Soc.* **2002**, *124*, 13194.
(38) Johnson, D. A.; Taylor, J. C.; Waugh, A. B. *J. Inorg. Nucl. Chem.* **1980**, *42*, 1271.
(39) Chisholm, M. H.; Folting, K.; Huffman, J. C.; Kirkpatrick, C. C. *Inorg. Chem.* **1984**, *23*, 1021.
(40) Berg, D. M.; Sharp, P. R. *Inorg. Chem.* **1987**, *26*, 2959.
(41) Clegg, W.; Errington, R. J.; Kraxner, P.; Redshaw, C. *J. Chem. Soc., Dalton Trans.* **1992**, 1431.

Table 1. Raman and IR Absorptions for 1, 2, 3a, 4a, and HOSi(O^{t}Bu)$_3$ and Tentative Assignments

1		**2**		**3a**		**4a**		HOSi(O^{t}Bu)$_3$		
Raman (cm^{-1})	IR (cm^{-1})	Raman (cm^{-1})	IR (cm^{-1})	Raman (cm^{-1})	IR (cm^{-1})	Raman (cm^{-1})	IR (cm^{-1})	Raman (cm^{-1})	IR (cm^{-1})	assignment[a]
1460 s		1460 s		1457 s		1458 s		1456 s		$\delta_{asym}(CH_3)$
1249 m	1244 s	1249 m	1244 s	1251 s	1250 m	1250 s	1244 s	1249 m	1248 s	ν(CC)
	1215 m		1215 m		1215 m		1217 sh			ν(CC)
1198 w	1190 s	1198 w	1196 s	1196 w	1190 s	1203 w	1195 s	1199 w	1198 s	$\rho(CCH_3)$
1086 s										ν(M═O)
1067 sh	1070 vs	1071 w	1074 s	1077 vw	1074 s		1072 s		1068 s	ν_{asym}(SiOC)
		1042 w				1040 w		1040 w		ν_{asym}(SiOC)
	1030 s	982 w	1032 s	1019 s	1031 m	951 s	1031 m			ν(M═O)
					1020 m		974 m			ν(M═O)
									1014 m	ν(CC)
976 w	964 m		970 m	958 m	955 m		960 m			Si−O−M
921 m	891 br, s	922 m	912 br, s	921 m	906 br, s	923 s	928 br, m	921 m	914 br, w	ν(SiO)
855 sh		891 w				871 w				
843 m	858 s	842 w	833 m	841 m	835 m	840 w	831 m	835 m	827 m	ν(CC)
813 s	806 w	815 m	806 vw	813 s	808 w	814 m	806 vw	806 m	798 w	ν(CC)
710 w	704 m	712 vw	704 s		706 s	710 vw	704 s			
651 w	650 w	649 m	646 vw	662 m	660 m	649 m	652 w			ν(MO)
546 w	552 vw	551 w	532 w	557 w	553 vw	551 w	540 w	628 s	627 m	δ(OSiO)
	511 w		513 sh		509 m		515 m		521 br, m	ν_{sym}(SiOC)
	501 m		499 m				498 m			
	476 m		476 m		476 s		480 m		486 br, m	δ_{asym}(SiOC)
	432 w		432 m		428 m		432 m		432 m	ν(CC)

[a] Abbreviations: v = very, s = strong, m = medium, w = weak, sh = shoulder, br = broad; ν = stretching, δ = deformation, ρ = rocking; sym = symmetric, asym = asymmetric.

significant decomposition occurs. The room-temperature ^{1}H and ^{13}C NMR spectra for **3**, **3a**, **4**, and **4a** indicate a symmetrical structure with equivalent siloxide ligands.

Characterizations of Molybdenum Complexes. The solution ^{95}Mo NMR spectra were obtained at 26.08 MHz and chemical shifts were referenced to external aqueous 2 M Na_2MoO_4 at pH 11.[42] The spectrum of **1** consists of a single signal at −159 ppm ($\omega_{1/2}$ = 186 Hz). This chemical shift lies in the range observed for MoO^{4+} compounds (δ −610 to +185).[43] The compound **3a** exhibits a singlet at −156 ppm ($\omega_{1/2}$ = 173 Hz) in its ^{95}Mo NMR spectrum. Significant chemical shift differences have been observed for complexes of the MoO_2^{2+} group upon changing the donor atoms of the additional ligands (δ −219 to +630).[44,45] Negative chemical shifts occur for MoO_2^{2+} species ligated exclusively by O atoms.[44] The chemical shift of **3a** is at relatively high field compared to those assigned to dioxomolybdenum complexes containing siloxide ligands, such as $MoO_2[(c\text{-}C_6H_{11})_7(Si_7O_{11})(OTMS)]$ (δ −70.6, $\omega_{1/2}$ = 220 Hz).[18]

The ^{29}Si NMR spectra of **1** and **3a** contain resonances at −99.9 and −96.3 ppm, respectively. For comparison, the ^{29}Si NMR resonance for a related dioxo complex containing a bridging, bidentate silandiolate, $[O_2Mo(O_2Si^tBu_2)]_2$,[17] appears at −3.8 ppm, and the analogous shift for the compound $[O_2Mo(OSi^tBu_2)_2O]_2$[46] was observed at −10.2 ppm.

The UV−vis spectra of molybdenum complexes **1** and **3** in toluene contain narrow absorption bands at 296 and 284 nm, respectively, assigned to ligand-to-metal charge-transfer (LMCT) band. In general, absorption bands around 230 nm are attributed to octahedral and tetrahedral Mo(VI) centers.[47] Bands at 250−290 nm have been assigned to tetrahedral MoO_4 and bands at 270−320 nm to octahedral MoO_6 species.[11,48−52] The overlap in these band assignments renders UV−vis spectroscopy somewhat ineffective for the characterization of molybdenum coordination environments. In addition, Fournier et al. suggested that the UV band position is more heavily influenced by Mo-support interactions and the Mo dispersion than by the local symmetry at Mo.[49,53] Compound **3** exhibits an absorption band at 284 nm, which is relatively high compared to that generally observed for tetrahedral Mo(VI) species. However, this band is in close proximity to that observed for **1** (296 nm). Thus, as suggested by Fournier, the Mo coordination geometry seems to have a rather small influence on the UV−vis band position.

Raman spectroscopy has proven to be a useful technique for the characterization of structures for surface-bound metal oxo species. For this reason, it was of interest to examine the Raman spectra of compounds **1** and **3a**, since their MoO-$[OSiO_3]_4$ and $MoO_2[OSiO_3]_2$ cores should mimic those of isolated oxo-molybdenum groups on silica. However, the vibrational modes for such species may be influenced by coupling to surface modes.[54] Assignments of the bands may be aided by comparisons with the Raman spectrum for HOSi-

(42) Masters, A. F.; Brownlee, R. T. C.; O'Connor, M. J.; Wedd, A. G.; Cotton, J. D. *J. Organomet. Chem.* **1980**, *195*, C17.
(43) Minelli, M.; Enemark, J. H.; Brownlee, R. T. C.; O'Connor, M. J.; Wedd, A. G. *Coord. Chem. Rev.* **1985**, *68*, 169.
(44) Christensen, K. A.; Miller, P. E.; Minelli, M.; Rockway, T. W.; Enemark, J. H. *Inorg. Chim. Acta* **1981**, *56*, L27.
(45) Minelli, M.; Yamanouchi, K.; Enemark, J. H.; Subramanian, P.; Kaul, B. B.; Spence, J. T. *Inorg. Chem.* **1984**, *23*, 2554.
(46) Gosink, H.-J.; Roesky, H. W.; Schmidt, H.-G.; Noltemeyer, M.; Irmer, E.; Herbst-Irmer, R. *Organometallics* **1994**, *13*, 3420.
(47) Jezlorowski, H.; Knozinger, H. *J. Phys. Chem.* **1979**, *83*, 1166.
(48) Rana, R. K.; Viswanathan, B. *Catal. Lett.* **1998**, *52*, 25.
(49) Fournier, M.; Louis, C.; Che M.; Chaquin, P.; Masure D. *J. Catal.* **1989**, *119*, 400.
(50) Iwasawa, Y.; Ogasawara, S. *J. Chem. Soc., Faraday Trans. 1* **1979**, *75*, 1465.
(51) Gajardo, P.; Grange, P.; Delmon, B. *J. Phys. Chem.* **1979**, *83*, 1771.
(52) Gajardo, P.; Pirotte, D.; Grange, P.; Delmon, B. *J. Phys. Chem.* **1979**, *83*, 1780.
(53) Hanna, T. A.; Ghosh, A. K.; Ibarra, C.; Mendex-Rojas, M. A.; Rheingold, A. L.; Watson, W. H. *Inorg. Chem.* **2004**, *43*, 1511.
(54) Magg, N.; Immaraporn, B.; Giorgi, J. B.; Schroeder, T.; Bäumer, M.; Döbler, J.; Wu, Z.; Kondratenko, E.; Cherian, M.; Baerns, M.; Stair, P.; Sauer, J.; Freund, H.-J. *J. Catal.* **2004**, *226*, 88.

$(O^tBu)_3$ (Table 1) and by previous assignments for the spectra of $MoOX_4$ and MoO_2X_2 (X = F, Cl, or Br).[55−57] Most apparent in the Raman spectrum of **1** is an intense band at 1086 cm^{-1}, which can be assigned to the Mo═O stretching mode of the O═MoO_4 moiety. The main feature of the spectrum of **3a** is a band at 1019 cm^{-1}, which can also be assigned to a Mo═O stretching mode. These bands therefore reflect a generally observed trend, which is that the vibrational frequency associated with a L_nMoO_2 dioxo structure is lower than that for a related L_nMoO monooxo species.[58] This assignment is in agreement with those reported for MoO_2X_2 (X = Cl, Br)[57] and $[O_2Mo(O_2Si^tBu_2)]_2$.[59] The less intense bands at 1067 cm^{-1} (in **1**) and 1077 cm^{-1} (in **3a**) may be due to an asymmetric Si−O−C stretching vibration. The related band in $HOSi(O^tBu)_3$ appears to be observed at 1040 cm^{-1}.[28,60] Pairs of bands at 921 and 546 cm^{-1} (in **1**) and 921 and 557 cm^{-1} (in **3a**) may correspond to Si−O stretching vibrations, as observed at 921 and 628 cm^{-1} in $HOSi(O^tBu)_3$.[28,60,61]

Hardcastle and Wachs have developed correlations between molybdenum−oxygen bond distances and the corresponding Raman stretching frequencies for a series of reference molybdenum compounds.[62] Application of these correlations to the 1086 and 651 cm^{-1} bands of **1** provides values of 1.65(2) and 1.89(2) Å for the Mo═O and Mo−O bond distances, respectively. These values are close to those expected on the basis of comparisons to related molybdenum complexes. For example, $MoO(OMe)_4$ possesses bond distances of 1.672(5) and 1.880(6) Å for the Mo═O and Mo−O bonds, respectively. For **3a**, the correlations yield 1.68(2) and 1.88(2) Å for the Mo═O and Mo−O bond distances, respectively. For comparison, the Mo═O and Mo−O bond lengths for $MoO_2(OSiPh_3)_2$ are 1.692(7) and 1.815(5) Å, respectively.[15]

The infrared spectra of **1**, **3a**, and $HOSi(O^tBu)_3$ are compared in Table 1. The most intense infrared peak in all the spectra is assigned as the Si−O−C stretching band at ca. 1070 cm^{-1}, which compares well to the assignment made for this band in the Raman spectra (1067 cm^{-1} for **1** and 1077 cm^{-1} for **3a**). Many bands in the IR spectrum of **1** can be assigned to the $-OSi(O^tBu)_3$ ligands, but two bands at 1030 and 964 cm^{-1} are unique to the IR spectrum of **1** and are assigned to vibrational mods for the Mo═O and Mo−O−Si linkages, respectively. Previously, a peak at ca. 940−970 cm^{-1} in the spectra of molybdenum-containing silica has been attributed to Si−O−H[63,64] or Si−O−Mo[65] groups or to a combination of both vibrations.[48,66] From our IR spectroscopic results, the intensity of the Si−O−H bending vibration (914 cm^{-1}) in the spectrum of $HOSi(O^tBu)_3$ is relatively weak compared to that of the Si−O−Mo vibration in the spectrum of **1**. Thus, we propose that the Si−O−H bonding vibration may not significantly contribute to this band in the spectrum of molybdena−silica materials with low concentrations of SiOH sites.

The infrared spectrum of **3a** exhibits two overlapping bands at 1020 and 1031 cm^{-1}, which were assigned to the Mo═O stretch. These values are significantly higher than those for the corresponding stretches observed for $MoO_2(OSiPh_3)_2$ (948 and 932 cm^{-1})[15] but are very similar to the corresponding values in $[O_2Mo(O_2Si^tBu_2)]_2$ (1020 cm^{-1}).[59] In addition, they correspond closely to the band assigned to this stretch in the Raman spectrum (1019 cm^{-1}).

Characterizations of Tungsten Complexes. The solution ^{183}W NMR spectra were acquired at 20.84 MHz and chemical shifts were referenced to external saturated aqueous Na_2WO_4 at pH 9.1.[67] The ^{183}W NMR spectrum of **2** exhibits a sharp single peak at +565.8 ppm. The chemical shift range for ^{183}W is in excess of 10 000 ppm, and the resonance position is strongly dependent on the coordination environment.[43] The chemical shift of **2** lies within the known window for tungsten in the VI oxidation state;[68] however, the chemical shifts for W(VI) species with similar bonding environments are more upfield. For example, the ^{183}W NMR resonances of $WO(O^tBu)_4$ and $WO(OMe)_4$ were observed at −386.9 and −62.9 ppm, respectively.[41] Thus, there is a marked downfield shift on replacing alkoxide ligands with $-OSi(O^tBu)_3$ groups. Macchioni et al.[69] observed a downfield shift upon a decrease in the coordination number from 6 to 5 (dimeric vs monomeric W(VI) imido compounds). Thus, the downfield shift found in **2** may result from a lower coordination number, since the complexes $WO(O^tBu)_4$ and $WO(OMe)_4$ are thought to exist as dimers.[41] Attempts to obtain a ^{183}W NMR spectrum of **4a** failed to achieve an acceptable S/N ratio before the compound decomposed. The ^{29}Si NMR spectra of **2** and **4a** exhibit chemical shifts at −98.5 and −88.8 ppm, respectively. These values are at relatively high field compared to the ^{29}Si NMR resonance for the Si−O−W group of $WO\{O(Ph_2SiO)_3\}_2(THF)$ (at −40.5 ppm)[19] but in the region expected for a $Si(OSi)_3(OM)$ center.[70,71]

The UV−vis spectra of **2** and **4a** in toluene contain a narrow absorption band at 284 nm, assigned to an O→W LMCT band. By comparing the spectra of W/HZSM-5 and W/SiO_2 with tungsten compounds of known geometry, de Lucas et al.[72,73] proposed that a band at 220 nm could be assigned to tetrahedrally coordinated W(VI), bands at 250−

(55) Alexander, L. E.; Beattie, I. R.; Bukovszky, A.; Jones, P. J.; Marsden, C. J.; Van Schalkwyk, B. J. *J. Chem. Soc., Dalton Trans.* **1974**, 81.
(56) Collin, R. J.; Griffith, W. P.; Pawson, D. *J. Mol. Struct.* **1973**, *19*, 531.
(57) Adams, D. M.; Churchill, R. G. *J. Chem. Soc. A* **1968**, 2310.
(58) Desikan, A. N.; Huang, L.; Oyama, S. T. *J. Phys. Chem.* **1991**, *95*, 10050.
(59) Haoudi-Mazzah, A.; Dhamelincourt, P.; Mazzah, A.; Lazraq, M. *J. Raman Spectrosc.* **1998**, *29*, 1047.
(60) Beckmann, J.; Dakternieks, D.; Duthie, A.; Larchin, M. L.; Tiekink, E. R. T. *Appl. Organomet. Chem.* **2003**, *17*, 52.
(61) Barraclough, C. G.; Bradley, D. C.; Lewis, J.; Thomas, I. M. *J. Chem. Soc.* **1961**, 2601.
(62) Hardcastle, F. D.; Wachs, I. E. *J. Raman Spectrosc.* **1990**, *21*, 683.
(63) Boccuzzi, F.; Coluccia, S.; Ghiotti, G.; Morterra, C.; Zecchina, A. *J. Phys. Chem.* **1978**, *82*, 1298.
(64) Neumann, R.; Levin-Elad, M. *J. Catal.* **1997**, *166*, 206.
(65) Raghavan, P. S.; Ramaswamy, V.; Upadhya, T. T.; Sudalai, A.; Ramaswamy, A. V.; Sivasanker, S. *J. Mol. Catal. A* **1997**, *122*, 75.
(66) Arnold, U.; Serpa da Cruz, R.; Mandelli, D.; Schuchardt, U. *J. Mol. Catal. A* **2001**, *165*, 149.
(67) Acerete, R.; Hammer, C. F.; Baker, L. C. W. *J. Am. Chem. Soc.* **1979**, *101*, 267.
(68) Mann, B. E. *Annu. Rep. NMR Spectrosc.* **1991**, *23*, 161.
(69) Macchioni, A.; Pregosin, P. S.; Ruegger, H.; van Koten, G.; Van der Schaaf, P. A.; Abbenhuis, R. A. T. M. *Magn. Reson. Chem.* **1994**, *32*, 235.
(70) Lippmaa, E.; Magi, M.; Samoson, A.; Engelhardt, G.; Grimmer, A.-R. *J. Am. Chem. Soc.* **1980**, *102*, 4889.
(71) Miller, J. M.; Lakshmi, L. J. *J. Phys. Chem. B* **1998**, *102*, 6465.

325 nm to octahedral species, and a band at 390 nm to bulk WO_3. The coordination geometry of tungsten in **4a** is likely to be octahedral; thus, the observed spectrum is consistent with the literature.

Transition-metal oxides, because of their structural symmetry, are generally very strong Raman scatterers.[74] For this reason, Raman spectroscopy has been widely used to identify condensed transition-metal oxide phases in the characterization of various transition-metal-containing composites. The Raman absorptions of **2** and **4a** are listed in Table 1. By comparing Raman data for WOX_4 and WO_2X_2 (X = F, Cl),[55,75,76] the bands at 982 and 951 cm^{-1} were assigned to the W═O stretching modes in **2** and **4a**, respectively. These assignments are in good agreement with those reported for silica-supported tungsten materials. For example, the Raman spectra of isolated oxo-tungsten on SiO_2 under anhydrous conditions display bands at 982−984 cm^{-1}.[8]

The IR spectra of **2** and **4a** exhibit very similar features to those of **1** and **3a**, respectively (Table 1), and display the expected resonances for the $-OSi(O^tBu)_3$ ligands. Compound **2** displays a band in the IR spectrum at 1032 cm^{-1}, which was assigned to the W═O stretching vibration. Two IR active W═O modes appearing at 1031 and 974 cm^{-1} confirm the presence of a *cis*-$[WO_2]^{2+}$ center in **4a**. These values are in the region for stretching modes reported for surface W═O groups in W-containing mixed oxides under anhydrous conditions (1015−1030 cm^{-1}).[77] However, they are significantly higher than those observed for $WO\{O(Ph_2SiO)_3\}_2$(THF) (968 cm^{-1}) and $WO_2(OSiPh_3)_2(OSC_4H_8)_2$ (945 and 893 cm^{-1})[19] and approach those observed in halide complexes.[75,76]

Thermolytic Behavior of 1, 2, 3a, and 4a. The decomposition behavior of compounds **1**, **2**, **3a**, and **4a** was initially probed by thermal gravimetric analysis (TGA). The TGA trace for **1** under a flow of nitrogen shows an initial weight loss starting at only 50 °C and a decomposition process which becomes quite rapid at 80 °C. The observed ceramic yield at 1000 °C was 32.9%, which is in close agreement with the calculated yield for $MoO_3{\cdot}4SiO_2$ (33.0%).

Thermolysis of a benzene-d_6 solution of **1** (in a sealed NMR tube with ferrocene as an internal standard) at 150 °C led to elimination of 9.2 equiv of isobutene, 1.5 equiv of water, 0.15 equiv of $HOSi(O^tBu)_3$, and gel formation. This result should be compared with the expected yields for a clean thermolysis via isobutene elimination (eq 3). The lower than expected amount of water may be attributed to the low solubility of water in benzene or the presence of an oxide desiccant formed during the thermolysis.[30] The small amount of $HOSi(O^tBu)_3$ observed may be due to hydrolysis of precursor species by water as it forms in the reaction. A portion of isobutene is assumed to be present in the gas phase above the deuterated solvent. The molybdenum-containing material formed at this temperature should have an average composition of $MoSi_4O_{11}$.

$$MO[OSi(O^tBu)_3]_4 \xrightarrow{\Delta} MSi_4O_{11} + 6H_2O + 12CH_2{=}CMe_2 \qquad M = Mo\ (\mathbf{1}),\ W\ (\mathbf{2}) \quad (3)$$

The TGA results for **2** under flowing nitrogen reflect an onset temperature of ca. 100 °C and a weight loss that is complete by 200 °C. The ceramic yield of 35.1% is 2.6% lower than that expected for stoichiometric formation of $WO_3{\cdot}4SiO_2$ (37.7%) but is in good agreement with the formation of $WO_{1.5}{\cdot}4SiO_2$ (35.8%). In addition, the solid residue recovered after heating to 1000 °C was pale blue. This result implies that tungsten is reduced during the thermolysis under nitrogen. The TGA trace for **2** under flowing oxygen is similar to the one obtained under nitrogen, except that the ceramic yield of the off-white powder at 200 °C (38.6%) is higher and in agreement with the formation of $WO_3{\cdot}4SiO_2$. The decomposition of a benzene-d_6 solution of **2** was presumed to follow the process described by eq 3. Heating at 150 °C for 1 h resulted in complete conversion of **2**; the products observed were isobutene (8.7 equiv), water (1.5 equiv), $HOSi(O^tBu)_3$ (0.01 equiv), and HO^tBu (0.005 equiv). Prolonged heating at 170 °C did not lead to a significant change in this product mixture.

The TGA trace for **3a** exhibits an initial, precipitous weight loss occurring at ca. 70 °C. The thermolytic conversion process occurs in a stepwise fashion, with the first step completed by ca. 400 °C and resulting in a 37.6% ceramic yield, which approximately corresponds to the formation of $MoO_3{\cdot}2SiO_2$ (36.3%). The second weight loss, occurring between 650 and 1000 °C, is more gradual and appears to correspond to the sublimation of MoO_3.[78] The ceramic yield at 1000 °C (20.9%) was only 4.4% higher than that expected for $2SiO_2$ (16.5%). Thermolysis of a benzene-d_6 solution of **3a** at 150 °C resulted in the evolution of isobutene (2.3 equiv), water (0.4 equiv), HO^tBu (0.7 equiv), and THF (1.0 equiv). For comparison, the theoretical values for these elimination products are given in eq 4.

$$MO_2[OSi(O^tBu)_3]_2(L) \xrightarrow{\Delta} MSi_2O_7 + 3H_2O + 6CH_2{=}CMe_2 + L \qquad M = Mo,\ L = THF\ (\mathbf{3a});\ M = W,\ L = DME\ (\mathbf{4a}) \quad (4)$$

The TGA trace for **4a** exhibits a gradual weight loss beginning near room temperature. At about 85 °C, the weight loss becomes more rapid and results in a ceramic yield of 45.1% at 1000 °C. This is slightly higher than the expected ceramic yield for $WO_3{\cdot}4SiO_2$ of 42.3%. The decomposition of a benzene-d_6 solution of **4a** occurred very readily. After heating the solution at 85 °C for 3 h, a gel was formed. The soluble decomposition products were determined to be

(72) de Lucas, A.; Valverde, J. L.; Canizares, P.; Rodriguez, L. *Appl. Catal. A* **1998**, *172*, 165.
(73) de Lucas, A.; Valverde, J. L.; Canizares, P.; Rodriguez, L. *Appl. Catal. A* **1999**, *184*, 143.
(74) Graselli, J. G.; Bulkin, B. J. *Analytical Raman Spectroscopy*; Wiley: New York, 1991.
(75) Ward, B. G.; Stafford, F. E. *Inorg. Chem.* **1968**, *7*, 2569.
(76) Beattie, I. R.; Livingstone, K. M. S.; Reynolds, D. J.; Ozin, g. A. *J. Chem. Soc. A* **1970**, 1210.
(77) Ramis, G.; Cristiani, C.; Elmi, A. S.; Villa, P.; Busca, G. *J. Mol. Catal.* **1990**, *61*, 319.
(78) Dazhuang, L.; Lixiong, Z.; Biguang, Y.; Jiaofeng, L. *Appl. Catal. A* **1993**, *105*, 185.

Table 2. Properties of the Xerogels Derived from 1, 2, 3a, and 4a

sample	calcination temperature (°C)	combustion analysis % C	combustion analysis % H	surface area ($m^2\ g^{-1}$)	pore volume ($cm^3\ g^{-1}$)
MoSi4		0.71	<0.2	10	0.05
MoSi4	300	<0.2	0.27	5.9	0.05
MoSi2		8.38	0.77	100	0.5
MoSi2	300	0.7	<0.2	110	0.5
WSi4		2.10	<0.2	230	0.8
WSi4	300	1.12	<0.2	230	0.8
WSi2		3.11	0.66	270	0.8
WSi2	300	1.43	<0.2	260	0.8

isobutene (5.6 equiv), ^{t}BuOH (1.0 equiv), water (0.4 equiv), and DME (1.0 equiv).

Xerogel Formations from 1, 2, 3a, and 4a. The facile thermal elimination of organic fragments from **1**, **2**, **3a**, and **4a** allowed the solution-phase formation of inorganic networks via thermolysis. Heating toluene solutions of **1**, **2**, **3a**, and **4a** to 180 °C in a sealed Parr reactor under a nitrogen atmosphere produced blue gels within 18 h. Upon air-drying, these gels shrank to ca. 30% of their original volume and became hard, pale blue materials. The pale blue color of these materials suggests that the Mo(VI) and W(VI) centers from the precursors were reduced during the thermolysis reactions. The gels were washed with pentane and then air-dried for another 24 h. The final xerogels were ground into fine powders and dried at 120 °C under reduced pressure for 18 h to provide the as-prepared materials: **MoSi4** (from **1**), **WSi4** (from **2**), **MoSi2** (from **3a**), and **WSi2** (from **4a**).

Elemental analyses of the as-prepared **MoSi4** and **MoSi2** revealed Mo/Si molar ratios of 0.27 and 0.50, respectively, which correspond very closely to the expected ratios (0.25 and 0.50) and indicate that the original stoichiometry of the precursors are retained upon thermal conversion to Mo/Si/O materials. Similarly, the as-prepared **WSi4** and **WSi2** have W/Si ratios of 0.26 and 0.51, respectively. The organic contents of these as-prepared materials are shown in Table 2. Calcination to 300 °C under a flow of oxygen removed most of these organic residues as determined by combustion analyses.

Thermogravimetric analyses of the as-prepared **MoSi4** and **MoSi2** materials under a flow of oxygen revealed further weight losses of up to 15% through 700 °C, attributed to dehydration and condensation of the network as well as removal of any organic residues and water. In addition, the material changed color from blue to white at ca. 300 °C, suggesting the presence of only the fully oxidized Mo(VI) at this temperature. Above 700 °C, the TGA results of **MoSi4** and **MoSi2** revealed a significant weight loss of 14.3% and 37.5%, respectively, perhaps because of partial sublimation of MoO_3.[78] The TGA results for the as-prepared **WSi4** and **WSi2** revealed weight losses of up to 10% through 1000 °C (under oxygen), which are consistent with the organic contents determined by elemental analyses (Table 2). The as-prepared **WSi4** and **WSi2** materials changed color from blue to off-white at ca. 300 °C. The off-white color persisted until ca. 600 °C when the powder became pale yellow. The yellow color, associated with crystalline WO_3, continuously intensified until 1000 °C. The changes of colors suggest that the W reduced centers in the as-prepared **WSi4** and **WSi2** materials were oxidized during the heating under oxygen.

The crystallization behavior of **MoSi4**, **WSi4**, **MoSi2**, and **WSi2** as a function of temperature was studied by powder X-ray diffraction (PXRD). The as-prepared samples **MoSi4** and **MoSi2** were amorphous by PXRD, but heating to 400 °C for 3 h under a flow of oxygen (heating rate of 10 °C min^{-1}) induced the crystallization of MoO_3. The crystallinity of **MoSi2** (calcined at 400 °C) was higher than that of **MoSi4**, as indicated by the PXRD pattern. These results are possibly due to the higher molybdenum content in **MoSi2**, which may facilitate the crystallite formation. After the samples were heated to 500 °C under oxygen, the crystallites of **MoSi2** increased in size to ca. 45 nm, as approximated by the Scherrer equation.[79] The low temperature at which MoO_3 crystallizes in **MoSi4** and **MoSi2** suggests that the xerogel may not be atomically well-mixed or that the diffusion of molybdenum species is quite facile. Even though the blue color of the as-prepared **WSi4** and **WSi2** suggests a presence of the reduced W centers, no other W species than hexagonal WO_3 phase was detected by PXRD. After calcinations to 300 °C, peaks corresponding to crystalline WO_3 sharpen and increase in intensity. The crystallinity of **WSi2** was higher than that of **WSi4**, as observed for the molybdenum analogues. Heating **WSi2** under oxygen at 500 °C yielded a mixture of hexagonal and monoclinic WO_3. The presence of the crystalline WO_3 indicates that disproportionation of the W−O−Si linkages of the precursor into W−O−W and Si−O−Si connectivities during the thermolysis process is relatively facile. The Raman spectra of the as-prepared **WSi4** and **WSi2** also confirm the presence of WO_3 domains, with bands at 810 and 720 cm^{-1}.[80]

Infrared spectra of **MoSi4** and **MoSi2** (Figure 4a in the Supporting Information) resemble those of molybdenum-substituted silicates.[64−66] The IR spectra exhibit strong Si−O−Si stretches at 1080 and 1180 (broad shoulder) cm^{-1} and lattice vibrations for silica at 460 and 575 cm^{-1}. Raman spectroscopy is much more sensitive than PXRD (detection limit of ca. 50 Å) in the detection of MoO_3 domains. The Raman spectra of uncalcined **MoSi4** and **MoSi2** are presented in Figure 4b (Supporting Information). Peaks at ca. 1000, 825, and 680 cm^{-1} are attributed to the formation of MoO_3 in the silica matrix.[11,58] These results were also supported by DRUV−vis spectroscopy. MoO_3 exhibits an adsorption maximum at 330 cm^{-1} in the DRUV−vis spectrum,[11] and broad absorption bands at 300 and 320 nm were observed for **MoSi4** and **MoSi2**, respectively. The low dispersity of metal centers in **MoSi4**, **WSi4**, **MoSi2**, and **WSi2** is presumably a result of the high metal loading.

Nitrogen porosimetry was used to further evaluate the pore structures and surface areas of the **MoSi4**, **WSi4**, **MoSi2**, and **WSi2** materials (Table 2). All samples exhibit a type IV N_2 isotherm with a H3 hysteresis, which is indicative of a tenuous assemblage of particles that define slit-shaped pores.[81,82] The corresponding pore size distributions are quite broad with pore radii ranging from 5 to 1000 Å. Additionally, the as-prepared **MoSi4** has a surprisingly low surface area of 10 m^2g^{-1} compared to the surface of 106 m^2g^{-1} in the

(79) Scherrer, P. *Gotting. Nachr.* **1918**, *2*, 98.
(80) Zhang, Z.; Suo, J.; Zhang, X.; Li, S. *Appl. Catal. A* **1999**, *179*, 11.
(81) Sing, K. S. W.; Everett, D. H.; Haul, R.; Moscou, L.; Pierotti, R. A.; Rouquerol, J.; Siemieniewska, T. *Pure Appl. Chem.* **1985**, *57*, 603.
(82) Gregg, S. J.; Sing, K. S. W. *Adsorption, Surface Area and Porosity*, 2nd ed.; Academic Press Inc.: London, 1982.

Scheme 2

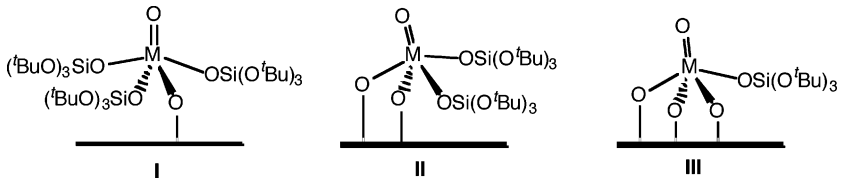

as-prepared **MoSi2**. This result is counter-intuitive, considering the larger amount of silica present in **MoSi4**. The as-prepared **WSi4** and **WSi2** have surface areas of 230 and 270 m^2g^{-1}, respectively. These surface areas are quite high, considering the presence of the crystalline WO_3 detected by PXRD in the samples. Calcinations of these as-prepared materials to 300 °C under a flow of oxygen resulted in essentially no change in surface areas or pore volumes (Table 2).

Grafting of 1 and 2 onto SBA-15. The precursor complexes **1** and **2** were grafted onto the mesoporous SBA-15 support by stirring a suspension of the support in a hexane solution of the precursor for 19 h at ambient temperature. Any unreacted precursor and byproducts from the grafting reaction were removed by filtration and washing of the resulting solid with hexane. The metal content of the resulting materials is in close agreement with the stoichiometries employed in the synthetic procedures. The samples prepared from **1** and **2** are denoted **Mo/SBA-15** and **W/SBA-15**, respectively. The maximum metal loadings (obtained by employing a large excess of the corresponding precursor) were 1.85 wt % **Mo/SBA-15** (0.22 Mo/nm^2) and 3.34 wt % **W/SBA-15** (0.22 W/nm^2). The maximum metal coverages are similar to those achieved by grafting (^{i}PrO)Ti[OSi(O^{t}Bu)$_3$]$_3$ (0.28 Ti/nm^2)[36] and Fe[OSi(O^{t}Bu)$_3$]$_3$(THF) (0.26 Fe/nm^2)[37] onto SBA-15.

The chemical reactions associated with the grafting process were monitored by ^{1}H NMR spectroscopy. The reactions of the precursors with silica were expected to proceed via a displacement of the siloxide ligands by surface hydroxyl groups.[36,37,83] The major product from the grafting reactions of **1** and **2** in benzene-d_6 was identified by ^{1}H NMR spectroscopy as HOSi(O^{t}Bu)$_3$. Only a trace amount of HO^{t}Bu was detected in the grafting reaction of **1**, and none was detected in the grafting reaction of **2**. Thus, these precursors appear to bind to the surface exclusively via reactions of the siloxide ligand.

The ^{1}H NMR spectroscopic studies of the grafting reactions suggest the formation of structures involving bonding interactions between the silica surface and each molybdenum or tungsten center (Scheme 2). Comparisons of the consumption of the precursors and the production of HOSi(O^{t}Bu)$_3$ during the grafting process provide some evidence for the predominant structure for the grafted metal species, as 0.7−1.0 equiv of HOSi(O^{t}Bu)$_3$ was recovered from preparative scale grafting reactions. Also by elemental analysis, the carbon and hydrogen contents (Table 3) are consistent with a structure with one bonding interaction between the silica and the metal center (type I in Scheme 2).

(83) Roveda, C.; Church, T. L.; Alper, H.; Scott, S. L. *Chem. Mater.* **2000**, *12*, 857.

Table 3. C and H Elemental Analysis Results for 1.02 wt % Mo/SBA-15 and 1.64 wt % W/Sba-15

sample	possible structure	theor values of C, H (%)	obsd C and H elemental anal. (%)
1.02 wt % **Mo/SBA-15**	Type I (Scheme 2)	C: 4.60, H: 0.87	C: 4.51, H: 0.85
	Type II	C: 3.06, H: 0.58	
1.64 wt % **W/SBA-15**	Type I	C: 3.86, H: 0.73	C: 5.10, H: 1.19
	Type II	C: 2.57, H: 0.49	

Thermogravimetric analyses of the grafted samples revealed a precipitous weight loss through 400 °C corresponding closely to organic contents found by elemental analyses. The PXRD and N_2 adsorption indicate that the regular structures of the SBA-15 support remain intact after the grafting procedures. Furthermore, the intensity of the hydroxyl band (ca. 3700 cm^{-1}) associated with the silica surface in the IR spectra is considerably attenuated upon the introduction of **1** or **2**. Evidence from these IR spectroscopic results suggests that the attachment of the precursor molecules was predominantly via ligand displacement. Calcinations of **Mo/SBA-15** and **W/SBA-15** to 500 °C for 6 h under a flow of oxygen did not affect the pore structures and did not result in formation of MoO_3 or WO_3 domains as determined by PXRD. Additionally, the lack of the characteristic absorption bands for MoO_3 and WO_3 in IR and Raman spectra of **Mo/SBA-15** and **W/SBA-15** further confirm the absence of MoO_3 and WO_3 domains in the corresponding materials. However, the vibrations ascribed to the M−O−Si linkages remain unresolved, perhaps because of the low metal loadings and the thickness of the SBA-15 walls. The DRUV−vis spectra of the uncalcined 1.49 wt % **Mo/SBA-15** and 3.34 wt % **W/SBA-15** resemble the UV−vis spectra of their corresponding precursors with λ_{max} values of 285 and 274 nm, respectively. Calcination of these samples to 500 °C in situ did not change these λ_{max} values, suggesting no change to the local environment of the metal centers.

Catalytic Oxidation of Cyclohexene. Samples of **1**, **2**, **MoSi4**, **MoSi2**, **WSi4**, **WSi2**, **Mo/SBA-15**, and **W/SBA-15** were investigated as catalysts in the oxidation of cyclohexene with *tert*-butyl hydroperoxide (TBHP) or aqueous hydrogen peroxide (30% H_2O_2) as the oxidant. It was found that the molecular precursors **1** and **2** in toluene at 65 °C are active and selective homogeneous catalysts for the epoxidation of cyclohexene with TBHP as the oxidant. After 1 h, the cyclohexene oxide yields were 49.3 and 6.3% (relative to initial peroxide) for **1** and **2**, respectively. These conversions correspond to 28 and 3 turnovers, respectively. In addition, the selectivities toward the production of cyclohexene oxide were greater than 99%. However, both molecular precursors underwent decomposition as solid precipitates appeared after the first hour of their catalytic reaction.

Samples of **MoSi4**, **MoSi2**, **WSi4**, **WSi2**, **Mo/SBA-15**, and **W/SBA-15** exhibited activity as catalysts for the

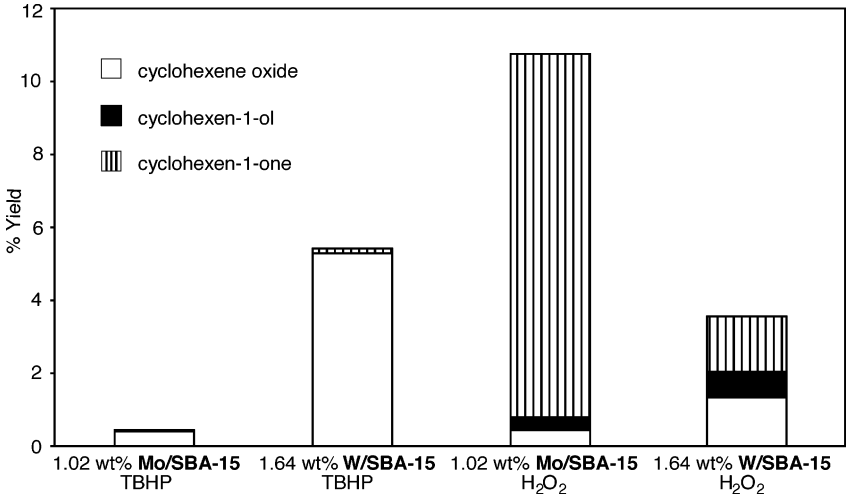

Figure 1. Yield of cyclohexene oxidation products, cyclohexene oxide, cyclohexen-1-ol, and cyclohexen-1-one, at 2 h relative to initial oxidant, TBHP or H_2O_2, with 1.02 wt % **Mo/SBA-15** or 1.64 wt % **W/SBA-15** catalysts.

oxidation of cyclohexene with TBHP or H_2O_2 as the oxidant. In general, the initial cyclohexene oxide production is rapid over the first 30 min of the reaction, and a reduced rate is observed thereafter. This is attributed to the increase in quantities of water or alcohol coproducts in the reaction mixture, thereby hindering formation of the active metal−peroxide complexes and the subsequent reaction with cyclohexene.[84] In control experiments with **MoSi4** or 1.02 wt % **Mo/SBA-15** catalyst and no oxidant, or with oxidant and no catalyst, no cyclohexene oxidation products were observed by gas chromatography (GC) analysis after 2 h.

Xerogels **MoSi4** and **MoSi2** (calcined to 300 °C under oxygen) were active catalysts with TBHP as the oxidant at 65 °C in toluene and yielded 48.5 and 34.0% cyclohexene oxide after 2 h, respectively. These catalysts were 100% selective toward the production of cyclohexene oxide after a reaction time of 2 h (% selectivity = $100([\text{epoxide}]_t/[\text{epoxide}]_i - [\text{epoxide}]_t)$, where t is the reaction time). The production of cyclohexene oxide is greater for **MoSi4** than for **MoSi2** (both per mass of catalyst and per Mo basis), despite the surface area of **MoSi4** being ca. 100 m^2g^{-1} less. This may be due to a higher concentration of inactive molybdenum species in **MoSi2**, which may result from its high molybdenum content. With H_2O_2 as the oxidant, the reactivity was very low and it appeared that molybdenum species leached into solution (by visual observation of the solution color). Both **WSi4** and **WSi2** exhibited a very similar reactivity and were only slightly active in the epoxidation of cyclyhexene with TBHP, yielding only 2.0 and 1.9% cyclohexene oxide after 2 h, respectively.

The **Mo/SBA-15** and **W/SBA-15** materials were active in the oxidation of cyclohexene at 65 °C in toluene with TBHP as the oxidant (Figure 1). Unlike the titanium-based catalysts (SBA-15 supported $Ti[OSi(O^tBu)_3]_4$),[36] calcination does not have a significant effect on the catalysts' activities. The as-prepared 1.49 wt % **Mo/SBA-15** afforded 8.7% epoxide after 2 h, while the calcined **Mo/SBA-15** yielded 9.6% epoxide in the oxidation of cyclohexene with TBHP. Thus, only materials that had been calcined to 500 °C for 6 h under a flow of oxygen were further studied. The oxidation of cyclohexene with TBHP at 65 °C in toluene (with 1.02 wt % **Mo/SBA-15** or 1.64 wt % **W/SBA-15** catalyst) proceeded with high selectivity (>98% at 2 h), but at a low rate. After 2 h, the conversions were only 8.0 and 5.4% for 1.02 wt % **Mo/SBA-15** and 1.64 wt % **W/SBA-15**, respectively. In addition, the recyclability of **Mo/SBA-15** was studied by using the catalyst in a second reaction run. Before being reused, the catalyst was separated from the reaction mixture by filtration at the reaction temperature, was washed with hexane, and was dried under vacuum at room temperature. A decrease in activity was observed in the second run (4.4 vs 7.9% epoxide yield), and this is possibly due to the deactivation of the molybdenum species during the first run.

Experiments employing H_2O_2 in acetonitrile at 65 °C revealed significantly different activities in the oxidation of cyclohexene (Figure 1). The 1.02 wt % **Mo/SBA-15** and 1.64 wt % **W/SBA-15** catalysts were active in the oxidation of cyclohexene; however, the major product was cyclohexen-1-one. After 2 h, the yields of cyclohexene oxide were 0.5 and 1.4% while those of cyclohexen-1-one were 9.9 and 1.5%, with 1.02 wt % **Mo/SBA-15** or 1.64 wt % **W/SBA-15** catalysts, respectively. To determine whether the active species leached into solution during a typical catalytic run, a sample of 1.02 wt % **Mo/SBA-15** with TBHP in toluene or with H_2O_2 in acetonitrile was heated to 65 °C for 1 h with rapid stirring. The mixture was then filtered via cannula while still hot, and the filtrate was treated with cyclohexene at 65 °C. Samples taken from this reaction mixture after 2 h contained no cyclohexene oxidation product, indicating that leaching of a catalytically active molybdenum species had not occurred. However, we cannot rule out the possibility that catalytically inactive species have leached into solution.

To make comparisons between the different systems studied here, the catalyst activities in turnover frequencies (TOFs), defined as moles of epoxide produced per mole of metal per hour, were determined. Figure 2a illustrates the catalyst activities in the epoxidation of cyclohexene with TBHP in toluene at 65 °C. The supported catalysts, **Mo/SBA-15** and **W/SBA-15**, have a very similar activity profile. The initial rate of cyclohexene oxidation was much greater

(84) Sheldon, R. A. *J. Mol. Catal.* **1980**, *7*, 107.

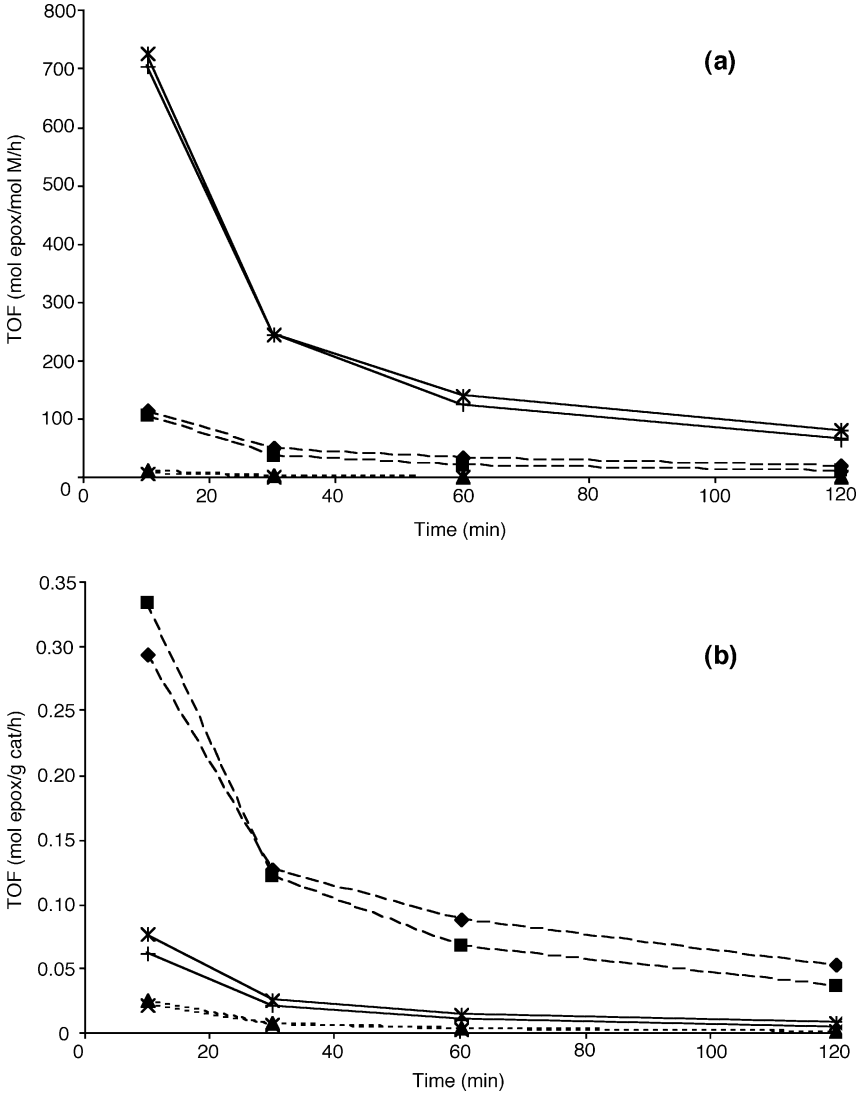

Figure 2. Turnover frequencies (TOFs) as a function of time during the epoxidation of cyclohexene with **MoSi4** (◆), **MoSi2** (■), **WSi4** (▲), **WSi2** (×), 1.02 wt % **Mo/SBA-15** (∗), and 1.64 wt % **W/SBA-15** (+). (a) TOF = moles cyclohexene oxide per moles M(VI) per hour. (b) TOF = moles cyclohexene oxide per gram catalyst per hour.

for the SBA-15 supported catalysts versus the xerogels. However, this comparison can be misleading, as it assumes that all of the metals in the catalysts are equally accessible for reaction with the substrates. It is only reasonable for the metal−supported catalysts, **Mo/SBA-15** and **W/SBA-15**, to assume that all of the metal centers are available for the reaction, whereas for the xerogel materials, **MoSi4**, **MoSi2**, **WSi4**, and **WSi2**, the metals are located throughout the bulk of the material. Therefore, it may be better to compare the TOFs of the different catalyst systems in terms of the mass of the catalyst (Figure 2b). In these comparisons, we see that **MoSi4** and **MoSi2** are better catalysts than **Mo/SBA-15** and **W/SBA-15**, while **WSi4** and **WSi2** are less active. However, the activities of **WSi4** and **WSi2** became comparable to those of **W/SBA-15** after the first hour of the epoxidation.

Concluding Remarks

The oxo-molybdenum and -tungsten siloxide complexes **1**−**4a** provide good spectroscopic models for isolated oxo-molybdenum and -tungsten on silica. Characterization data for these complexes offer benchmarks for spectroscopic studies of isolated oxo-molydenum and -tungsten sites on silica. Related molecular models based on molybdenum and tungsten siloxide complexes, such as $MoO_2(OSiPh_3)_2$,[15] $[O_2Mo(O_2Si^tBu_2)]_2$,[17] $WO\{O(Ph_2SiO)_3\}_2(THF)$, and $WO_2(OSiPh_3)_2(OSC_4H_8)_2$,[19] have been investigated, but these compounds possess Si−C bonds which tend to complicate their spectroscopic properties.

In this study, we have shown that the molecular complexes **1**−**4a** serve as relatively clean and efficient precursors for the preparation of metal oxide−silica composite materials, **MoSi4**, **MoSi2**, **WSi4**, and **WSi2**. However, the materials formed from thermolysis of **1**−**4a** in toluene do not consist of isolated molybdenum or tungsten in a matrix of silica but contain MoO_3 or WO_3 nanodomains, as shown by PXRD, Raman, and DRUV−vis spectroscopies. Thus, unlike in several other cases,[22,23,25,27,29,30] the single-source molecular precursors do not afford highly dispersed mixed-element samples. However, it may be possible to produce more well-dispersed Mo/SiO_2 and W/SiO_2 samples by increasing the silica content via cothermolyses of **1**−**4a** with $HOSi(O^tBu)_3$ as a silica source.[85]

The compounds **1** and **2** also appear to be useful for the introduction of molybdenum and tungsten centers, respectively, onto the mesoporous SBA-15 surface. Subsequent calcinations to 500 °C removed the organic groups from the grafted species while the mesoporous structures were maintained. A good dispersion of metal centers on the SBA-15 surface was achieved, as no MoO_3 or WO_3 aggregation was observed by PXRD, IR, Raman, and DRUV−vis spectroscopies.

The materials **MoSi4**, **MoSi2**, **WSi4**, **WSi2**, **Mo/SBA-15**, and **W/SBA-15** were investigated as epoxidation catalysts and were found to be active in the oxidation of cyclohexene. All materials were highly selective in the production of cyclohexene oxide (>95%) when TBHP was used as the oxidant. Using aqueous H_2O_2 as the oxidant, however, greatly reduced the cyclohexene oxide selectivities. In general, the molybdenum-containing catalysts are more active than the tungsten-containing ones. Furthermore, among the catalysts studied here, the molybdenum sites in **Mo/SBA-15** were the most active in the epoxidation of cyclohexene with TBHP in toluene at 65 °C. Although they are not exceptional catalysts for the epoxidation of cyclohexene, these materials may have applications in selective oxidations of other hydrocarbons.

Experimental Section

All manipulations were performed under an atmosphere of nitrogen with standard Schlenk techniques and in a Vacuum Atmospheres drybox. Dry oxygen-free solvents were used throughout. Calcinations were performed with a Lindberg 1200 °C three-zone tube furnace. NMR spectra were recorded on a Bruker AV300 (at 300 (^{1}H) MHz), AVB400 (at 26.1 (^{95}Mo) MHz), DRX500 (at 125.8 (^{13}C) or 99.4 (^{29}Si) MHz), or AV500 (at 20.8 (^{183}W) MHz). Infrared spectra were acquired as Nujol mulls with CsI cells on a Mattson Infinity Series FTIR spectrometer. Surface area and pore volume analyses were measured by using the BET method on a QuantaChrome Autosorb-1 surface area analyzer with all samples heated at 120 °C, under vacuum, for a minimum of 2 h immediately prior to data collection. Powder X-ray diffraction was performed on a Siemens D5000 diffractometer with Cu Kα radiation of wavelength 1.54056 Å. DRUV−vis spectra were recorded on a Varian Cary 4 UV−vis spectrometer with MgO as a reference. UV−vis measurements in solution were performed on a Hewlett-Packard 89532A diode array spectrophotometer. Raman spectra were recorded by Hololab series 5000 from Kaiser Optical Systems Inc., using a laser (60 mW, 532 nm). GC anyalyses were performed with a Hewlet Packard HP 6890 Series GC system using a methyl siloxane capillary (50.0 m × 320 μm × 1.05 μm nominal), and integration was performed relative to an internal standard (dodecane). Elemental analyses were performed by Galbraith Laboratories (Mo, W, and Si) or the College of Chemistry's Microanalytical Facility at the University of California, Berkeley (C and H). The starting materials $HOSi(O^tBu)_3$,[86] MoO_2Cl_2(dme),[87] WO_2Cl_2(dme),[88] and SBA-15[89] were prepared according to the literature procedures. All reagents were purchased from Aldrich and used as received, unless stated otherwise.

$LiOSi(O^tBu)_3$. A 1.6 M solution of ^{n}BuLi in hexane (30.0 mL, 48.0 mmol) was added dropwise to a cooled (0 °C) solution of $HOSi(O^tBu)_3$ (12.7 g, 48.0 mmol) in diethyl ether (75 mL). The reaction mixture was then allowed to warm and was stirred at room temperature for 20 h. The volatile materials were removed in vacuo, and the product was redissolved in pentane. Concentration and cooling (−30 °C) of the resulting solution yielded $LiOSi(O^tBu)_3$ in 81% yield (10.5 g). Anal. calcd for $C_{12}H_{27}O_4SiLi$: C, 53.06; H, 10.01. Found C, 53.04; H, 10.08. ^{1}H NMR (300 MHz, benzene-d_6): δ 1.53 (s, 27H, OCMe_3).

$MoO[OSi(O^tBu)_3]_4$ (1). A solution of $MoOCl_4$ (0.250 g, 0.988 mmol) in Et_2O (30 mL) was cooled to −78 °C in a dry ice/^{i}PrOH bath and a solution of $LiOSi(O^tBu)_3$ (1.06 g, 3.94 mmol) in Et_2O (30 mL) was added dropwise. The mixture was allowed to slowly warm to room temperature and was stirred for a total of 3 h. The volatile materials were removed in vacuo and the product was extracted from the LiCl with pentane (3 × 20 mL). Recrystallization (3×) from pentane at −30 °C afforded **1** as pale yellow crystals (10−42%). Anal. calcd for $C_{48}H_{108}O_{17}Si_4Mo$: C, 49.46; H, 9.64. Found C, 49.33; H, 9.69. ^{1}H NMR (300 MHz, benzene-d_6): δ 1.56 (s, 108H, OCMe_3).^{13}C{^{1}H} NMR (125.8 MHz, benzene-d_6): δ 73.6 (s, O*C*Me$_3$), 32.4 (s, OCMe_3). ^{29}Si NMR (99.35 MHz, benzene-d_6): δ −99.86 (s, O*Si*$(O^tBu)_3$). ^{95}Mo NMR (26.08 MHz, benzene-d_6): δ −159. IR (Nujol mull, CsI, cm^{-1}): 1365 s, 1244 s, 1215 m, 1190 s, 1070 br vs, 1030 s, 964 m, 891 br s, 858 s, 806 w, 704 m, 650 w, 552 vw, 511 w, 501 m, 476 m, 432 w.

$WO[OSi(O^tBu)_3]_4$ (2). A solid mixture of $WOCl_4$ (0.500 g, 1.46 mmol) and $LiOSi(O^tBu)_3$ (1.58 g, 5.85 mmol) was dissolved in Et_2O (50 mL). The resulting reaction mixture was stirred at ambient temperature for 18 h. The volatile materials were removed under vacuum and the product was extracted from the LiCl with pentane (3 × 20 mL). Concentration and cooling to −30 °C afforded **2** as a white powder (39%). Anal. calcd for $C_{48}H_{108}O_{17}Si_4W$: C, 45.99; H, 8.68. Found C, 45.61; H, 8.93. ^{1}H NMR (300 MHz, benzene-d_6): δ 1.56 (s, 108H, OCMe_3). ^{13}C{^{1}H} NMR (125.8 MHz, benzene-d_6): δ 73.7 (s, O*C*Me$_3$), 32.4 (s, OCMe_3). ^{29}Si NMR (99.35 MHz, benzene-d_6): δ −98.47 (s, O*Si*$(O^tBu)_3$). ^{183}W NMR (20.84 MHz, benzene-d_6): δ 565.8. IR (Nujol mull, CsI, cm^{-1}): 1366 s, 1244 s, 1215 m, 1196 s, 1074 br s, 1032 s, 970 m, 912 br s, 833 m, 806 vw, 704 s, 646 vw, 532w, 513 sh, 499 m, 476 m, 432 m.

$MoO_2[OSi(O^tBu)_3]_2$ (3). A solution of freshly prepared MoO_2Cl_2(DME) (1.00 g, 3.46 mmol) in Et_2O (30 mL) was cooled to −78 °C in a dry ice/^{i}PrOH bath and a solution of $LiOSi(O^tBu)_3$ (1.87 g, 6.92 mmol) in Et_2O (30 mL) was added dropwise. The mixture was allowed to warm to room temperature and was then stirred for 24 h. The volatile materials were removed in vacuo and the product was extracted from the LiCl with pentane (3 × 25 mL). Concentration and cooling to −30 °C afforded **3** as colorless crystals (32%). Anal. calcd for $C_{24}H_{54}O_{10}Si_2Mo$: C, 44.02; H, 8.31. Found C, 43.90; H, 8.31. ^{1}H NMR (300 MHz, benzene-d_6): δ 1.38 (s, 54H, OCMe_3). ^{13}C{^{1}H} NMR (125.8 MHz, benzene-d_6): δ 74.3 (s, O*C*Me$_3$), 31.9 (s, OCMe_3). IR (Nujol CsI, cm^{-1}): 1367 s, 1243 m, 1189 s, 1078 vs, 1028 m, 951 s, 902 s, 834 w, 804 w, 721 w, 703 m, 661 w, 506 w, 473 w, 428 m.

$MoO_2[OSi(O^tBu)_3]_2$(THF) (3a). Recrystallization of **3** from THF at −30 °C afforded colorless crystals (30% from MoO_2Cl_2(DME)) that turned opaque on exposure to vacuum. Anal. calcd for $C_{28}H_{62}O_{11}Si_2Mo$: C, 46.27; H, 8.60. Found C, 46.59; H, 8.88. ^{1}H NMR (300 MHz, benzene-d_6): δ 3.57 (m, 4H, OCH_2); 1.41 (m, 4H, CH_2); 1.38 (s, 54H, OCMe_3). ^{13}C{^{1}H} NMR (125.8 MHz, benzene-d_6): δ 74.3 (s, O*C*Me$_3$), 66.2 (s, O*C*H$_2$), 31.9 (s, OCMe_3), 26.2 (s, *C*H$_2$).^{29}Si NMR (99.35 MHz, benzene-d_6): δ −96.34 (s,

(85) Brutchey, R. L.; Lugmair, C. G.; Schebaum, L. O.; Tilley, T. D. *J. Catal.* **2005**, *229*, 72.
(86) Abe, Y.; Kijima, I. *Bull. Chem. Soc. Jpn.* **1969**, *42*, 1118.
(87) Kamenar, B.; Penavic, M.; Korpar-Colig, B.; Markovic, B. *Inorg. Chim. Acta* **1982**, *65*, L245.
(88) Dreisch, K.; Andersson, C.; Stalhandske, C. *Polyhedron* **1991**, *10*, 2417.
(89) Zhao, D., Huo, Q.; Feng, J.; Chmelka, B. F.; Stucky, G. D. *J. Am. Chem. Soc.* **1998**, *120*, 6024.

O*Si*(O^tBu)$_3$). ^{95}Mo NMR (26.08 MHz, benzene-d_6): δ −156. IR (Nujol CsI, cm^{-1}): 1367 s, 1250 m, 1215 sh, 1190 s, 1074 br s, 1031 m, 1020 m, 955 m, 906 br s, 835 m, 808 w, 706 s, 660 m, 553 vw, 509 m, 476 s, 428 m.

$WO_2[OSi(O^tBu)_3]_2$ (4). A solution of freshly prepared WO_2Cl_2(DME) (0.500 g, 1.33 mmol) in Et_2O (30 mL) was cooled to −78 °C in a dry ice/^{i}PrOH bath and a solution of $LiOSi(O^tBu)_3$ (0.716 g, 2.65 mmol) in Et_2O (30 mL) was added dropwise. The mixture was allowed to warm to room temperature and was then stirred for a total of 3 h. The volatile materials were removed in vacuo and the product was extracted from the LiCl with pentane (3 × 20 mL). Concentration and cooling to −30 °C afforded pure **4** as colorless crystals (52%). ^{1}H NMR (300 MHz, benzene-d_6): δ 1.39 (s, 54H, OC*Me*$_3$).

$WO_2[OSi(O^tBu)_3]_2$(DME) (4a). Recrystallization of **4** from pentane/DME (1:1) at −30 °C afforded analytically pure **4a** (52% from WO_2Cl_2(DME)). Anal. calcd for $C_{28}H_{64}O_{12}Si_2W$: C, 40.38; H, 7.75. Found C, 40.08; H, 7.68. ^{1}H NMR (300 MHz, benzene-d_6): δ 3.34 (m, 4H, C*H*$_2$); 3.24 (m, 6H, OC*H*$_3$); 1.41 (s, 54H, OC*Me*$_3$). ^{13}C{^{1}H} NMR (125.8 MHz, benzene-d_6): δ 73.3 (s, O*C*Me$_3$), 72.7 (s, *C*H$_2$), 60.7 (s, OC*H*$_3$), 31.6 (s, OC*Me*$_3$).^{29}Si NMR (99.35 MHz, benzene-d_6): δ −88.77 (s, O*Si*(O^tBu)$_3$). IR (Nujol CsI, cm^{-1}): 1367 s, 1244 s, 1217 sh, 1196 s, 1072 br s, 1031 m, 974 m, 960 m, 945 m, 928 br m, 831 m, 806 vw, 704 s, 652 w, 540 w, 515 m, 498 m, 480 m, 432 m.

Xerogel Formations from 1, 2, 3a, and 4a. Representative solution thermolyses were carried out as follows: A 20-mL Parr reactor was charged with a toluene (5.0 mL) solution of either **1** (0.500 g, 0.429 mmol), **2** (0.500 g, 0.400 mmol), **3a** (0.500 g, 0.688 mmol), or **4a** (0.500 g, 0.600 mmol) in a glovebox (N_2 atmosphere). The reactor was then placed in a preheated oven at 180 °C for 18 h. The wet gel was removed and air-dried for ca. 72 h to form a xerogel. The xerogel was rinsed with pentane (2 × 5 mL) and was allowed to air-dry for another 24 h. The xerogel was then ground into a fine powder, dried in vacuo for 18 h at 120 °C, and stored under N_2 in a glovebox. The following xerogels were formed from **1**, **2**, **3a**, and **4a**, respectively: **MoSi4**, 0.164 g (32.8%); **MoSi2**, 0.190 g (38.0%); **WSi4**, 0.223 g (44.8%); **WSi2**, 0.27 g (54.0%). Calcinations of the xerogels were carried out in a Lindberg 1200 °C three-zone tube furnace under a flow of O_2 (150 mL min^{-1}). The heating rate was 10 °C min^{-1} and the final temperature was maintained for 3 h. All materials were heated at 120 °C for at least 18 h in vacuo and subsequently stored under N_2 after each calcination stage.

Grafting 1 and 2 onto SBA-15. To remove any physisorbed water before the grafting procedure, the SBA-15 support was dehydrated at 200 °C for 24 h under a dynamic vacuum. A 0.5-g sample of the support was suspended in hexane (25 mL). A hexane solution (25 mL) of **1** or **2** was prepared, the concentration of which depended on the desired metal loading. The precursor solution was then added to the SBA-15 suspension. The resulting mixture was stirred at room temperature for 19 h and then filtered and washed with hexane (3 × 25 mL). The grafted material was dried at room temperature under reduced pressure. Calcination of the sample was performed in a tube furnace under flowing oxygen. The temperature was ramped at a rate of 1 °C min^{-1} to 500 °C, and this temperature was maintained for 6 h. These samples are designated as **Mo/SBA-15** and **W/SBA-15**.

Catalysis Procedures. A sample of catalyst (0.025 g) was added to a 50-mL round-bottom flask. Toluene (5.00 mL) and distilled cyclohexene (1.00 mL, 9.88 mmol) were added by syringe through a septum under a flow of nitrogen. Dodecane (0.250 mL) was added as an internal standard via micropipet. The mixture was allowed to equilibrate at the reaction temperature of 65 °C for 10 min. *tert*-Butyl hydroperoxide (1.00 mL, 5.5 mmol) was added by syringe to the rapidly stirred solution. When aqueous hydrogen peroxide (0.50 mL, 4.4 mmol) was used as the oxidant, acetonitrile (5.00 mL) was used as a solvent. Aliquots (ca. 0.15 mL) were removed from the reaction mixture by syringe after 10, 30, 60, 120, 180, and 1440 min and then filtered. The filtrate was analyzed by GC, and assignments were made by comparison with authentic samples analyzed under the same conditions.

Acknowledgment. This work was supported by the Director, Office of Energy Research, Office of Basic Energy Sciences, Chemical Sciences Division, of the U.S. Department of Energy under Contract No. DE-AC03-76SF000098. J. J. thanks the Royal Thai Government for support with a DPST scholarship. We also thank Professors A. Stacy (PXRD) and E. Iglesia (DRUV-vis, Raman) for the use of instrumentation. We are grateful to Dr. H. van Halbeek for technical assistance with ^{95}Mo and ^{183}W NMR spectroscopy.

Supporting Information Available: TGA traces for **1** and **3a**, PXRD patterns for **MoSi4**, **MoSi2**, **WSi4**, and **WSi2**, IR and Raman spectra for **MoSi4** and **MoSi2**, and a plot of TBHP yields as a function of time (PDF). The material is available free of charge via the Internet at http:// pubs.acs.org.

CM040344E